

## ACTIVITY AND SELECTIVITY CONTROL IN IRON CATALYZED FISCHER-TROPSCH SYNTHESIS

THE INFLUENCE OF IRON CATALYST PHASE ON SLURRY FISCHER-TROPSCH REACTION PATHWAYS; SELECTIVE SYNTHESIS OF ALPHA-OLEFINS.

S. SOLED, E. IGLESIA

*Exxon Research and Engineering Company, Annandale, New Jersey 08801, U.S.A.*

R.A. FIATO

*Exxon Research and Engineering Company, Florham Park, New Jersey 07932, U.S.A.*

Carbon monoxide hydrogenation, Fischer-Tropsch synthesis, iron carbides, olefin synthesis, promoted iron catalysts, slurry reactors, synthesis gas conversion

We present results of a catalyst structure-function study that supports a CO hydrogenation model with  $\alpha$ -olefins formed as the principal primary products and n-paraffins formed during secondary hydrogenation reactions. The interplay of catalyst composition and reaction environment controls the extent of secondary reactions. Catalysts that contain mainly oxidic phases or carbides with large concentrations of excess “matrix carbon” favor secondary reactions. The relative concentrations of oxide and carbide phases depends on the ease of reduction of the catalyst, which can be changed by cation substitutions. For example, cobalt substitution into  $\text{Fe}_3\text{O}_4$  lowers the reduction temperature by 20 °C. Excess matrix carbon has been intentionally introduced (by treatment in high temperature  $\text{H}_2/\text{CO}$ ) into model iron carbide catalysts produced by laser synthesis. Increased paraffin selectivity as matrix carbon is introduced suggests the influence of the diffusion constraints on product selectivity. Alkali promotion will affect secondary hydrogenation pathways. We illustrate how catalysts with low levels of alkali become increasingly more selective to paraffins at high conversions (and high effective  $\text{H}_2/\text{CO}$  ratios).

Reaction environment also controls catalyst composition and selectivity. Mossbauer spectroscopy on spent catalysts suggests that oxide/carbide phase formation in iron catalysts are sensitive to reactor configuration (extent of backmixing). In integral fixed bed reactors, catalysts partition into carbide phases in the front of the bed but show increasing amounts of oxide near the exit, whereas the catalysts in the stirred tank reactor remain all carbides. Product selectivities reflect the phase differences.

Other examples illustrating secondary hydrogenation phenomena will be presented.

### 1. Introduction

Selectivity control remains a critical issue in Fischer-Tropsch chemistry. The ability to control the molecular weight distribution of the products, the relative

olefin/paraffin content, and deviations from Anderson-Schultz-Flory polymerization kinetics represent current areas of scientific and technological importance in a catalytic process that dates back more than fifty years [1].

Traditional Fischer-Tropsch synthesis using iron catalysts produces a wide range of paraffinic and olefinic products, ranging from methane to high molecular weight waxes. These catalysts exhibit a variable degree of water gas shift activity; in some cases this leads to 30–50% of the carbon feed being rejected as  $\text{CO}_2$ . In addition, the Boudouard reaction can result in deposition of carbon on the catalyst and generation of additional  $\text{CO}_2$ . Thermodynamics favors the formation of methane. Operating conditions can be adjusted to control selectivities but overall effects are limited [2–4].

During Fischer-Tropsch synthesis with conventional bulk iron catalysts, various phases, including metal, metal carbides and metal oxides are present at steady-state catalytic conditions. Controversy remains about the role of each of these phases in the working catalyst [5–7].

Previous studies indicate that alkali increases the heat of CO chemisorption while decreasing the heat of  $\text{H}_2$  chemisorption [8,9]. Alkali also increases both the CO saturation coverage, and the probability of dissociating CO upon heating [9]. As a result of alkali promotion on iron catalysts, the average chain length and the olefin content of the products increase, whereas the activity and methane selectivity decrease [10,11].

Recent studies continue to indicate that  $\alpha$ -olefins, the major primary products formed during Fischer-Tropsch synthesis, participate in secondary reactions [12]. As CO dissociates, carbidic intermediates formed on the surface are reduced with  $\text{H}_2$ , and can add to growing chains in a statistical mode approximated by Anderson-Schultz-Flory polymerization kinetics [13]. Chains can terminate either by  $\beta$ -hydrogen abstraction to form an  $\alpha$ -olefin or by H-addition to form a paraffin [14]. Olefins can undergo secondary reactions by subsequent readsorption leading to isomerization or hydrogenation.

The isothermal backmixed environment of a slurry reactor provides more uniform redox conditions throughout the catalyst sample. In contrast, a plug flow reactor creates significant redox gradients in the axial direction with a highly reducing inlet and an oxidizing outlet. Consequently, correlating phase composition and catalyst performance in a CSTR is more straightforward. In this paper, we describe the interplay of the catalyst redox chemistry, promoter influence, and product selectivities in a backmixed environment.

We observe selectivity relationships that are consistent with Egiebor's proposal that significant secondary hydrogenation reactions can occur on iron catalysts [12]. The secondary reactions change the selectivity from predominantly olefinic to paraffinic. Catalysts that contain mainly iron oxide as opposed to iron carbide favor secondary hydrogenation reactions. The steady state concentration of the oxide phase in the catalyst depends on reducibility, which is affected by cation substitution into  $\text{Fe}_3\text{O}_4$  or  $\text{Fe}_2\text{O}_3$ . For example, we show how cobalt substitution

into  $\text{Fe}_3\text{O}_4$  lowers the reduction temperature substantially. Iron carbides do not favor secondary hydrogenation reactions, but the presence of excess “matrix carbon” on the carbide increases olefin residence time within catalyst pellets and enhances secondary hydrogenation reactions. We have compared an iron carbide catalyst produced by laser synthesis and containing nearly stoichiometric  $\text{Fe}_3\text{C}$  against a similar catalyst treated at high temperature in  $\text{H}_2/\text{CO}$  to produce excess matrix carbon.

## 2. Experimental

Iron oxides in the form of the spinel  $\text{Fe}_3\text{O}_4$  were used. In some cases potassium carbonate was then impregnated by incipient wetness. The details of the preparation of the iron oxide catalyst precursors are described elsewhere [15–17]. For those carbides made by ex-situ carburization, the oxide was loaded into a 1” diameter quartz tube and heated in a 1/1  $\text{H}_2/\text{CO}$  mixture at a volume hourly space velocity of  $10,000 \text{ hr}^{-1}$  at  $350^\circ\text{C}$  for 24 hours. These catalysts were then passivated at room temperature in a 1%  $\text{O}_2$  in  $\text{N}_2$  stream before catalytic experiments. Iron carbide catalysts were also prepared by laser pyrolysis of iron carbonyl and ethylene using a 150 watt continuous wave  $\text{CO}_2$  laser to provide both a rapid high temperature reaction ( $\sim 0.1 \text{ sec}$  with  $T \sim 1000^\circ\text{C}$ ) and quench [18].

Catalyst tests were performed in a 300 cc stirred tank reactor with octacosane as the slurry medium. Gas feed rates were controlled by mass flow controllers; the pressure was maintained by a dome-loaded back pressure regulator. Typical operating conditions were  $270^\circ\text{C}$  and 600 kPa. In most runs a Hewlett Packard 5840-A refinery gas analyzer was used to sample inlet and exit gas containing a  $\text{N}_2$  internal calibration standard. Liquid products collected in a cold trap at  $0^\circ\text{C}$  were analyzed by injection into an HP 5880 capillary gas chromatograph.

Wide-angle powder X-ray diffraction identified catalyst phases present in both initial and steady state samples. Thermogravimetric reductions were recorded on a Mettler TA-2000C using 100–200 mg of sample and a heating rate of 8 deg/min. Gravimetric titrations were performed using a specially designed heated entry port enabled injection of the pyridine titrant [19].

Mössbauer spectra were collected with an Austin Sciences instrument with a radiation source consisting of  $^{57}\text{Co}$  diffused into Rh (New England Nuclear). A multichannel analyzer and computer fitting programs were used to collect and analyze the data.

## 3. Results and discussion

Unpromoted iron oxide catalysts (surface area  $30\text{--}50 \text{ m}^2/\text{gm}$ ) and iron oxide converted ex-situ to iron carbide were compared under standard reaction condi-

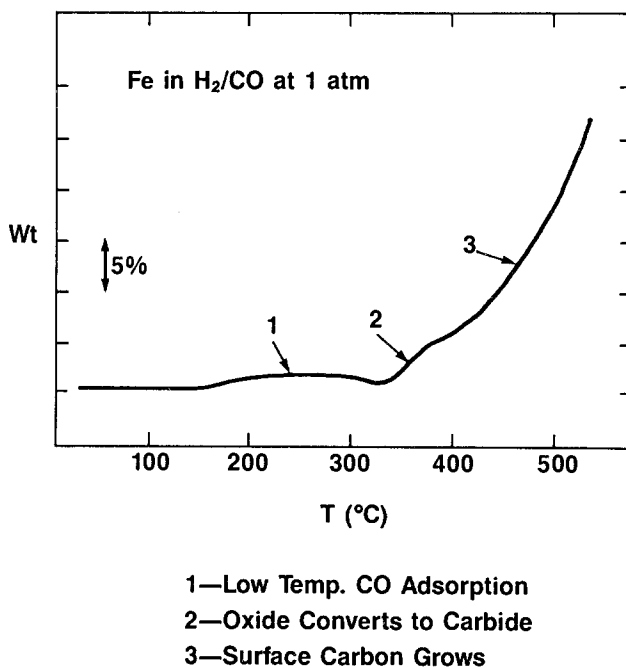


Fig. 1. Thermal conversion of iron to iron carbide.

tions. The analyzed carbon content following the 350 °C treatment in H<sub>2</sub>/CO was 40 wt% compared to a stoichiometric quantity of 7.9%, indicating formation of a substantial amount of excess matrix carbon. Fig. 1 illustrates the sequential conversion of an iron surface in 1 : 1 H<sub>2</sub> : CO at 1 atm under programmed heating conditions. In region 1 CO adsorbs onto the metal surface. At about 300 °C, Fe begins to convert to (Haag) carbide and at slighter higher temperature amorphous carbon begins to grow. After 60 hours of reaction at 270 °C and 600 kPa both the iron oxide and iron carbide catalyst retained their original bulk phase identity by X-ray. Although this does not rule out a minor surface conversion of the oxide, we would expect the appearance of iron carbide above ~ 5% level. Gravimetric acidity titrations with 3,5 dimethylpyridine at 250 °C showed an acid site concentration of 99 μmoles/gm catalyst for the oxide and only 27 for the carbided catalyst. These numbers compare with ~ 250 μmole/gm for a solid acid like γ-Al<sub>2</sub>O<sub>3</sub>. Consequently the acid site population on the oxide surface is substantial.

Fig. 2 summarizes the different product selectivities measured at conversions of ~ 50%. Space velocities in figs. 2 through 8 are reported in units of cm<sup>3</sup> of gas (at STP) per gram of catalyst per hour. Selectivities reflect secondary product formation. On the oxide catalyst all the ethylene has readsorbed and undergone secondary hydrogenation. This unsubstituted olefin most easily readsorbs because of its facile π-complex formation. In the carbided system we find ethylene

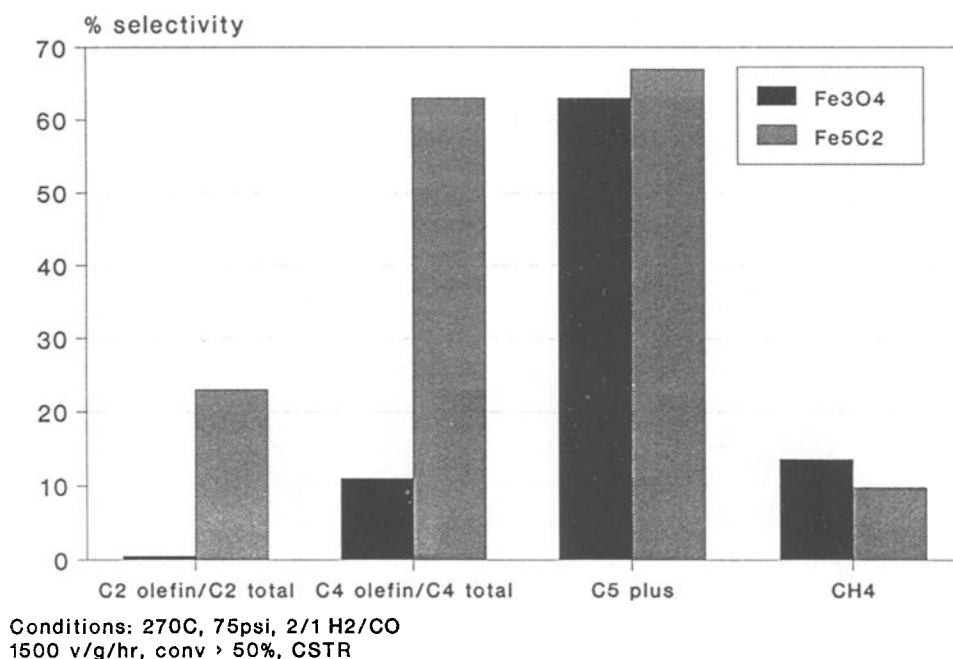
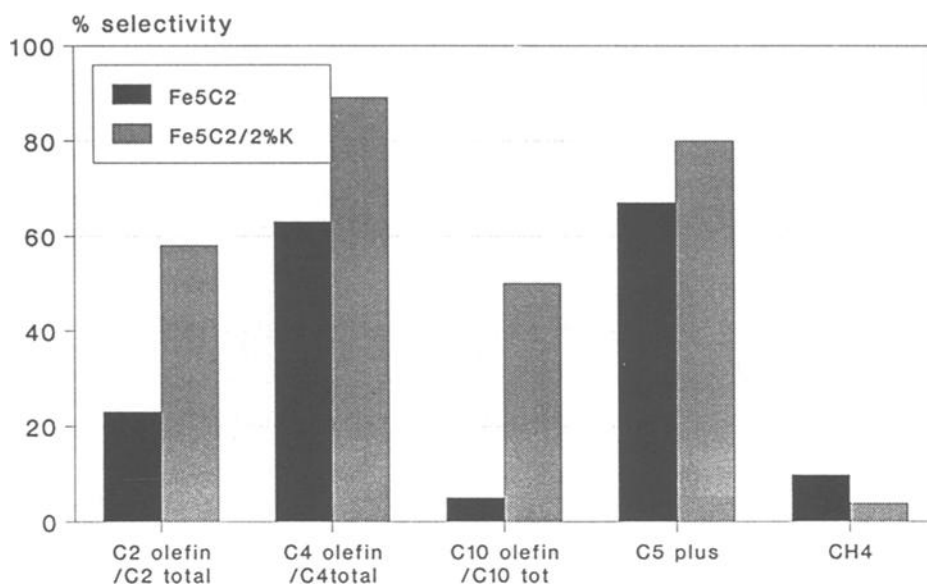


Fig. 2. Oxide surface shows more secondary products than carbided surface.

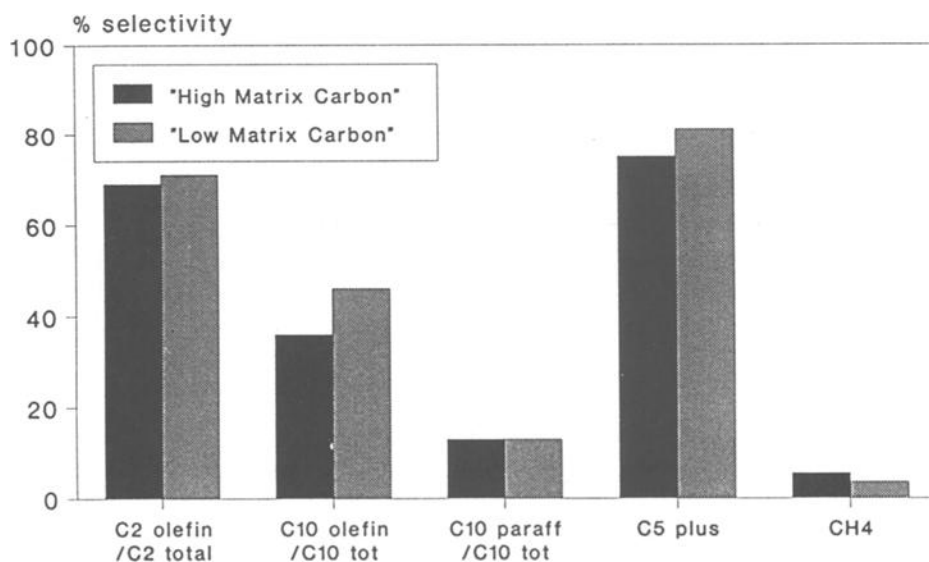
present as well as a higher olefinic content in C<sub>4</sub>, apparently as a result of inhibited secondary hydrogenation. The oxide surface also limits the extent of chain growth; the C<sub>5</sub> plus fraction is higher with the carbide. Consequently, a carbided iron surface produces a more olefinic, heavier product than an oxide surface. This is consistent with the observations of Egiebor and Cooper who suggest that acid sites on a precipitated FeO<sub>x</sub>/SiO<sub>2</sub> catalyst lead to a secondary reactions of  $\alpha$ -olefins [12]. We find that the more acidic oxide surface leads to secondary reactions.

Alkali titrates acid sites on the iron surface and also increases the strength of the CO-surface interaction. The latter results in a higher effective CO/H<sub>2</sub> surface ratio which in turn (i) increases olefinicity, (ii) increases average product molecular weight, (iii) decreases methane and (iv) decreases conversion. Fig. 3 compares the effect of potassium promotion on the iron carbide catalyst. The olefin selectivities have increased, methane selectivity decreased and the product has become heavier. In these carbided catalysts, however, we have substantial amounts of matrix carbon. A cementite Fe<sub>3</sub>C phase was synthesized by laser pyrolysis with a carbon content corresponding closely to the Fe<sub>3</sub>C stoichiometry; ie. without any excess matrix carbon. Some of it was heated in H<sub>2</sub>/CO mixtures (1/1) at 350 °C in order to introduce excess matrix carbon. The catalyst obtained now contained 40–50% by weight carbon. Fig. 4 shows that the excess carbon reduced olefin selectivity while favoring CH<sub>4</sub> and lighter products. It is also intriguing that this



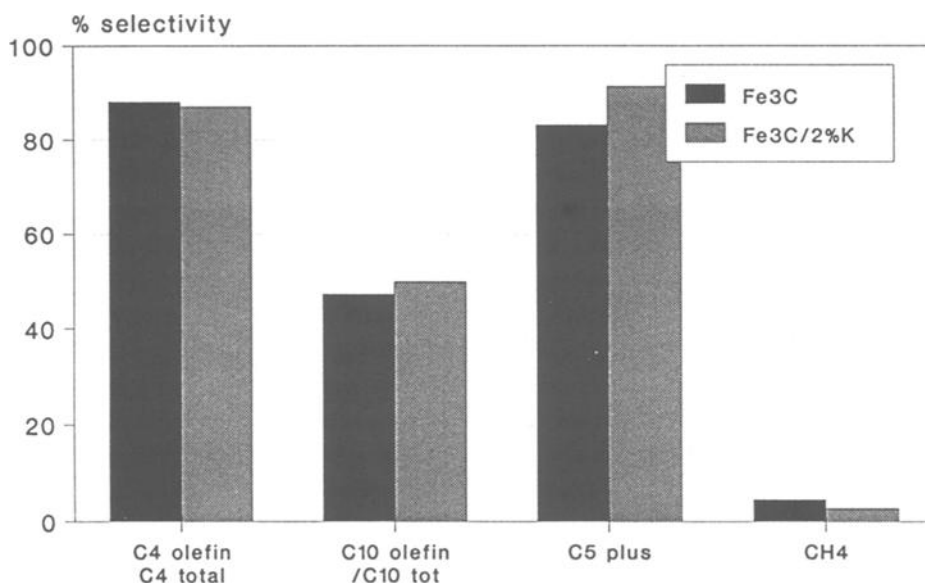
Conditions: 270C, 75 psi, 2/1 H<sub>2</sub>/CO  
1500 v/g/hr, conv >50%, CSTR

Fig. 3. Alkali promotion inhibits secondary hydrogenation.



Conditions: 270C, 75 psi, 2/1 H<sub>2</sub>/CO  
1000-8000 v/g/hr, CSTR  
*Laser Generated Catalysts*

Fig. 4. Excess matrix carbon decreases selectivity on laser generated Fe<sub>3</sub>C.



Conditions: 270C, 75 psi, 2/1 H<sub>2</sub>/CO  
8000 v/g/hr, CSTR

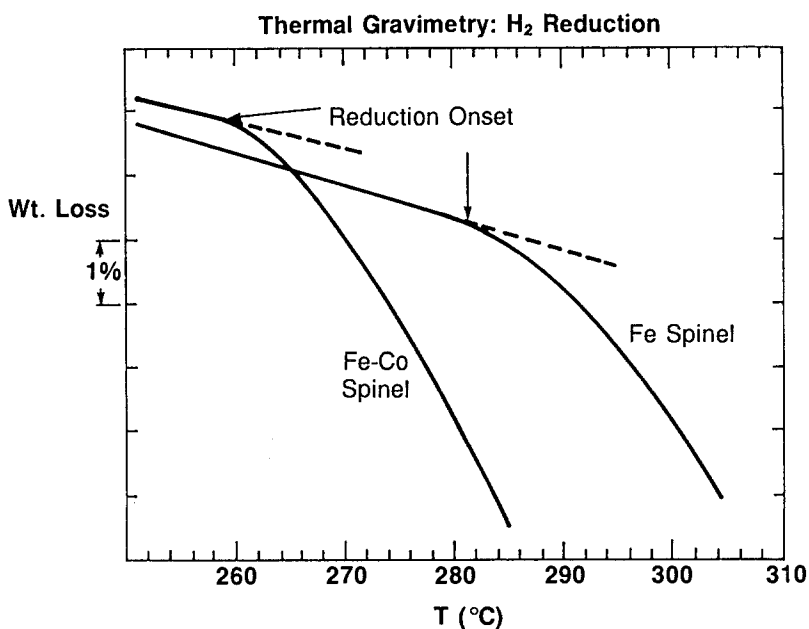
Fig. 5. Potassium promotion has minor effect on laser-generated iron carbides.

carbide as prepared does not respond to alkali treatment (fig. 5). This suggests that potassium is only needed when removal of the olefins is not fast enough to prevent secondary hydrogenation. This can occur in conventionally prepared catalysts when some residual acid sites remain.

The oxide catalyst reduces at lower temperature with substitution of Co into Fe<sub>3</sub>O<sub>4</sub>. Fig. 6 shows the onset of reduction is initiated 20 °C lower with the cobalt substitution. This may explain the enhanced olefin selectivity attributed to iron-cobalt relative to iron only catalysts in the literature [20,21], although cobalt alone is known to produce predominantly paraffins.

Reaction environment also controls catalyst composition and therefore selectivity. Mössbauer spectroscopy on spent catalysts suggests that oxide/carbide phase formation in iron catalysts is also sensitive to reactor configuration (extent of backmixing). In integral fixed bed reactors, we find that an iron catalyst has partitioned into iron carbide in the front of the bed but shows increasing amounts of oxide near the exit, whereas the same catalyst in the stirred tank reactor remains all iron carbide (fig. 7). Fig. 8 shows the rapid falloff in the alpha-olefin/n-paraffin ratio at C6 plus for the biphasic catalyst. Note that both the ethylene content as well as the C5 plus is lower on the oxide catalyst, paralleling the result described in fig. 2.

In the backmixed reactor the H<sub>2</sub>/CO ratio approximates that of the exit gas, so that at higher conversions with the water gas shift reaction occurring, a higher effective H<sub>2</sub>/CO ratio results. The effect of alkali loading also becomes evident in



- Onset of Reduction Lowered by 20°C with Co Substitution

Fig. 6. Cobalt substitution facilitates reduction of Fe<sub>3</sub>O<sub>4</sub>.

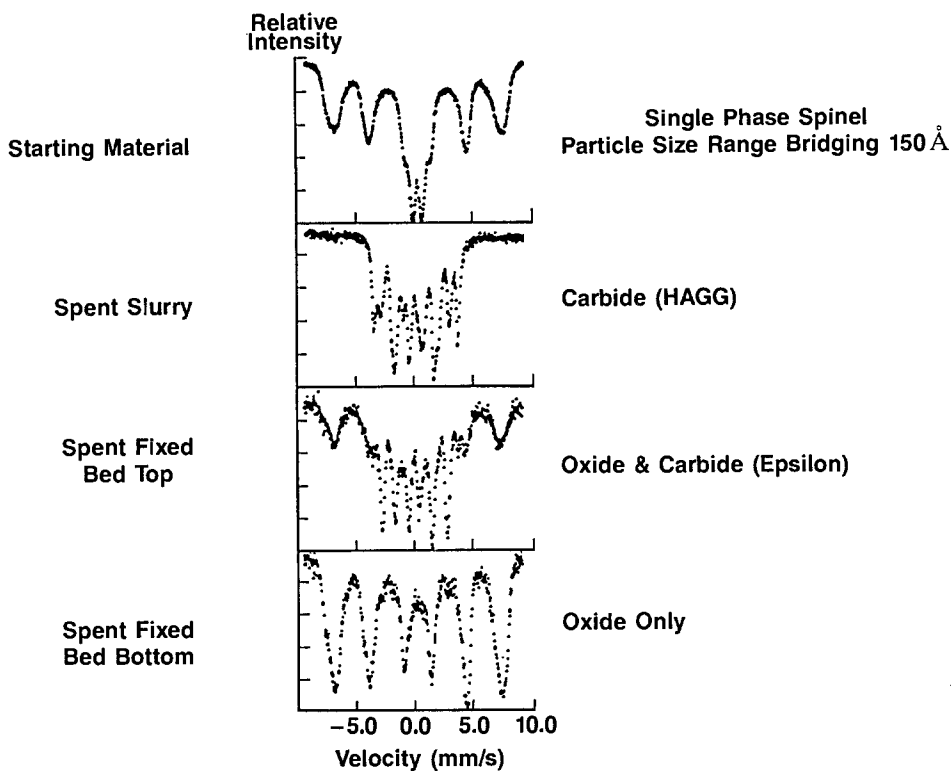
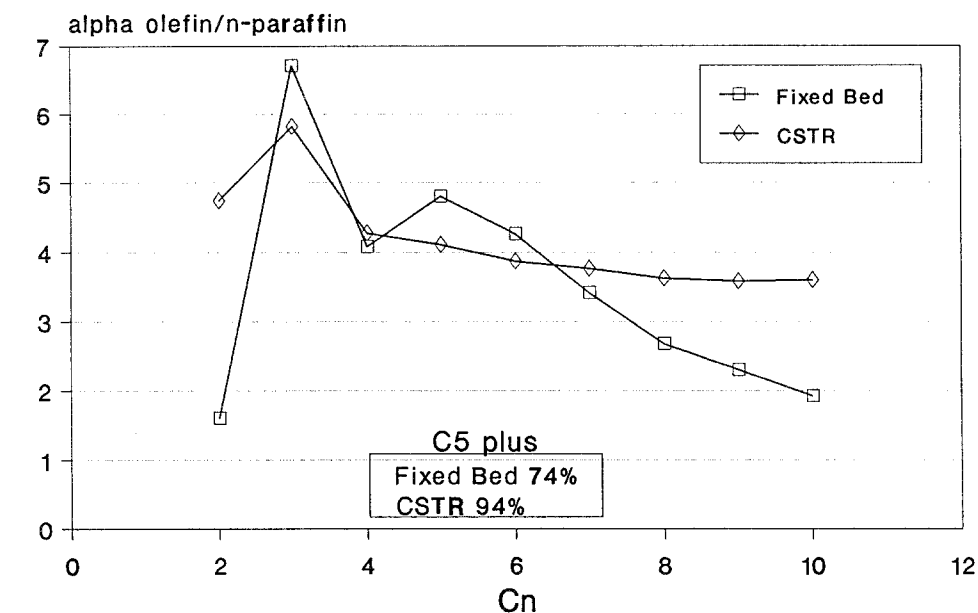


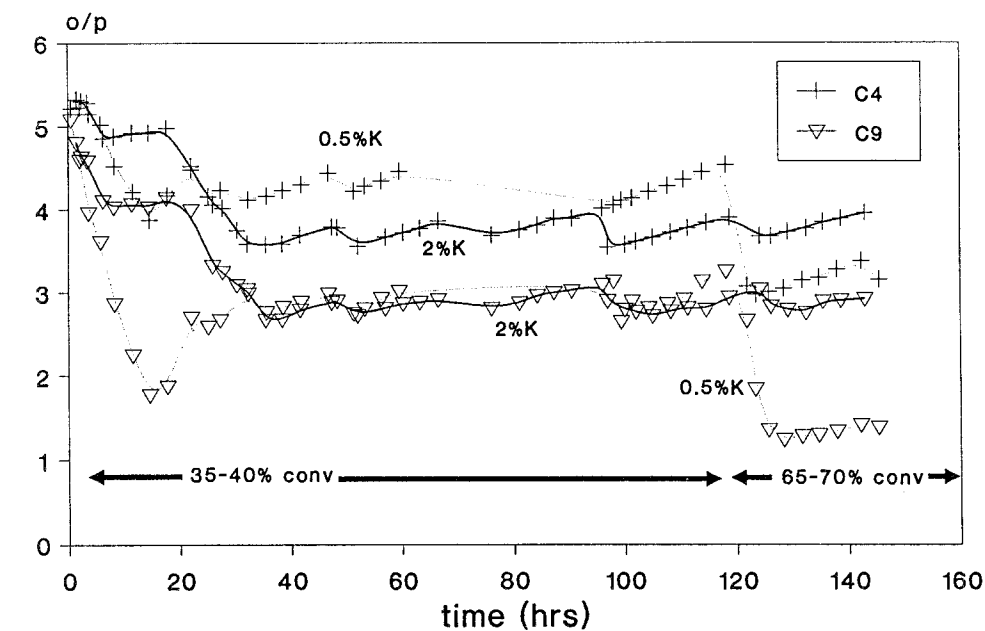
Fig. 7. Mössbauer spectroscopy reveals different phases present in slurry vs. fixed bed reactors.





270 C, 75 psi, 2/1 H<sub>2</sub>/CO, 10000 v/g/hr  
70-80 hr, conversion > 50%

Fig. 8. Alpha-olefin/n-paraffin ratio fixed bed vs CSTR.



Conditions: 270C, 75 psi, 2/1 H<sub>2</sub>/CO, CSTR

Fig. 9. Relative potassium loading effects selectivity at high conversion.

such a high conversion backmixed environment. For example, as we reduce the space velocity by a factor of two, the conversion increases from 40 to 70% as expected. The product olefinicity decreases with increasing conversion, ie. as the effective  $H_2/CO$  ratio increases, for the catalyst with low alkali. In contrast, the catalyst with high alkali maintains constant olefin selectivity under both low and high conversion conditions (fig. 9).

### Acknowledgements

The authors would like to thank Dr. Gary Rice for the preparation of the laser synthesized iron carbides and Dr. Carl Lund for the Mössbauer measurements.

### References

- [1] M.E. Dry, The Fischer-Tropsch Synthesis, in: *Catalysis, Science and Technology*, eds. J.R. Anderson and M. Boudart (NY, 1981) Vol. 1, p. 159.
- [2] C.D. Frohning and B. Cornils, Hydrocarbon Processing, (Nov. 1974) 143.
- [3] B. Cornils, B. Buessmeier and C.D. Frohning, Inf. Ser.-Alberta Res. Council 85 (1978) 126.
- [4] B. Buessmeier, C.D. Frohning and B. Cornils, Hydrocarbon Processing, (Nov. 1976) 105.
- [5] F. Fischer and H. Tropsch, Brennstoff-Chem. 7 (1926) 97.
- [6] V.V. Niemansverdriet, A.M. vander Kraan, W.L. Van Dyk and H.S. vander Baan, J. Phys. Chem. 84 (1980) 3363.
- [7] F. Balnchard, J.P. Reymond, B. Pommier and S.J. Teichner, *3rd Int. Symp. on Scient. Basis for Prep. of Het. Catal.* (Belg), Sept. 1983; and J. Mol. Catal. 176 (1982) 171.
- [8] M.E. Dry, T. Shingles, L.J. Boshoff and G.J. Ostuizien, J. Cat. 15 (1969) 190.
- [9] J. Benziger and R.J. Madix, Surf. Sci. 94 (1980) 119.
- [10] D.L. King and J.B. Peri, J. Cat. 79 (1983) 164.
- [11] H. Storch, N. Golumbic and R.B. Anderson, *Fischer-Tropsch and Related Synthesis* (Wiley N.Y., 1951) Ch. 6.
- [12] N.O. Egiebor and W.C. Cooper, Appl. Catal. 17 (1985) 47.
- [13] P. Biloen, J.N. Helle and W.M.H. Sachtler, J. Cat. 58 (1979) 95.
- [14] G. Henrici-Olive and S. Olive, Angew. Chem. Int. Ed. 15 (1976) 136.
- [15] R.A. Fiato and S.L. Soled, U.S. Pat. 4,618,597 (1986).
- [16] S.L. Soled and R.A. Fiato, U.S. Pat. 4,544,671 (1985).
- [17] S.L. Soled and R.A. Fiato, U.S. Pat. 4,584,323 (1986).
- [18] G. Rice, R.A. Fiato and S.L. Soled, U.S. Pat. 4,788,222 (1988).
- [19] S. Soled, G. McVicker and B. DeRites, *Proc. 11th North American Thermal Analysis Conf.*, 1981.
- [20] M. Nakamura, B.B. Wood, P.Y. Hou and H. Wise, *Proc. 7th Int. Conf. of Catal.*, part 7a, June '80.
- [21] R.M. Stanfield and W.N. Delgass, J. Cat. 72 (1981) 37.